Vibration-observation techniques for digital speckle-pattern interferometry

Katherine Creath

Optical Sciences Center, University of Arizona, Tucson, Arizona 85721

Gudmunn Å. Slettemoen

The Foundation of Scientific and Industrial Research, N-7034 NTH, Trondheim, Norway

Received January 21, 1985; accepted May 24, 1985

Vibration observation is a major application of digital speckle-pattern interferometry (DSPI), which is a variation on electronic speckle-pattern interferometry (ESPI). DSPI processes speckle patterns in a computer rather than with a frame grabber and analog electronics as in ESPI. A new method of observing vibration fringes is presented and compared with existing techniques as well as some variations on them. Fringe contrast and signal-to-noise ratio are used as a means of comparison since these quantities are dependent on the techniques used. This new technique involves continuously subtracting a reference frame containing only self-interference terms and no cross-interference term from the time-averaged data frames of the vibrating object. This reference frame is created by vibrating a reference mirror at a high amplitude while the object is at rest. Comparisons of calculated fringe contrast with four other observation methods show that this method yields extremely good fringe contrast. Experimental results are shown for this new technique as well as for the most commonly used vibration-observation technique. These results show that the new technique is far superior to all the other methods for moderately unstable objects, which may slowly drift or deform in time.

1. INTRODUCTION

Digital speckle-pattern interferometry (DSPI) is a type of nondestructive testing that is a variation on electronic speckle-pattern interferometry (ESPI).[1] ESPI was developed by combining the well-known techniques of holographic and speckle interferometry having an in-line reference beam and an image-plane hologram setup and following the methods of double-exposure holography.[2–10] The "electronic" in ESPI refers to the video electronics processing of speckle patterns. In DSPI, the speckle patterns are digitally processed in a computer. Rather than recording speckle patterns using a television (TV) camera followed by electronics and a television monitor, DSPI utilizes a diode-array camera interfaced to a computer to process the data.

Like ESPI, this technique records the primary interference patterns between the object and the reference beams of the interferometer.[9] This is in contrast to holographic interferometry, which relies on detecting secondary interference patterns. To produce secondary interference patterns in holographic interferometry, one primary interference pattern is recorded in a hologram. This hologram is then illuminated by a second primary interference pattern. When the hologram is viewed, the observer sees the interference between the two primary interferograms. This is a secondary interference pattern created by optically processing two primary interference patterns. In ESPI, the secondary interferogram is formed by electronic processing. Recording the primary interferograms eliminates an intermediate recording step and permits the direct comparison of different processing techniques.

The processing of primary interferograms in ESPI was developed both to yield the same fringe geometry as photographic techniques[4] and to enable these fringes to be displayed on a TV monitor. This processing is done by high-pass filtering, full-wave rectification, and squaring of the video signal passing from the TV camera to the TV monitor. For comparison (or deformation) measurements, a stored reference frame is continuously subtracted from the incoming data before the electronic processing. The processing done by DSPI is similar.[1] In single-frame measurements, filtering is done by subtracting local averages from the data. The displayed result is the square of these filtered data. For comparison measurements, a reference frame stored in memory is continuously subtracted from the incoming data, and then this difference is squared and displayed.

The secondary fringes seen in DSPI are not normal interference fringes but rather are correlation fringes representing the correlation among speckle patterns. The information that gives rise to these fringes is contained in the cross interference between the reference and the object beams for each speckle pattern. Vibration measurements usually include many periods of object motion within the integration time of the camera. Vibration fringes show the correlation among different speckle patterns for all positions of the object during vibration. These many patterns are added together during the integration time of the camera. Nodal areas where the object is stationary are visible as bright areas in the resulting secondary-fringe pattern. If the object is vibrating sinusoidally, the envelope for the finges will have a Bessel-function dependence.[6] To see these fringes, a slowly varying intensity must be subtracted by high-pass filtering. This will significantly enhance the fringe contrast. However, there is residual noise owing to the self-interference of both the object and the reference beams with themselves that is left after filtering.

0740-3232/85/101629-08$02.00

This paper describes a technique developed by the authors that retains the secondary-fringe envelope but subtracts the self-interference noise to enhance the fringe contrast significantly. The single-frame vibration-observation technique is compared with this new technique as well as with three other vibration-observation techniques. Plots of contrast versus vibration amplitude are shown for each of the techniques, and experimental results for the single frame and the new technique are presented. The techniques and theory presented in this paper are applicable to both ESPI and DSPI systems.

2. THEORY

In this paper different methods of vibration observation are compared. This comparison is made by calculating and plotting the contrast C to investigate the values of C for different methods of vibration analysis. The derivation of the signal-to-noise ratio for a single time-averaged frame is reviewed, followed by the signal-to-noise ratio for the difference of two frames of speckle-pattern data. This derivation utilizes many simplifying assumptions to provide simple expressions for these quantities. The general expression for the signal-to-noise ratio has been derived elsewhere.[4,7,9,11,12] This derivation assumes that the system has an infinite bandwidth, so that the incident intensities are recorded instantaneously with no time delays caused by the electronics. It also assumes that the TV camera fully resolves the speckle pattern, that the directions of object illumination and viewing are parallel, and that the object motion is normal to the viewing direction.

The significant quantity in comparing different vibration-analysis techniques is the monitor fringe contrast or visibility. It is usually defined as

$$C = \frac{B_{\max} - B_{\min}}{B_{\max} + B_{\min}}, \tag{1}$$

where B is the brightness of the display monitor. Ideally, the brightness minimum should go to zero to yield the highest contrast possible. With $B_{\max}$ equal to the signal plus the noise and $B_{\min}$ equal to the noise, the contrast may be written as

$$C = \frac{S}{S + 2N} = \frac{\alpha}{\alpha + 2},$$

where S is the signal, N is the noise, and α is the signal-to-noise ratio.

In ESPI the primary interference between a speckle object beam and specular reference beam is recorded by a camera. The specular reference beam has a complex amplitude $A_R = |A_R| \exp[i\phi_R]$. The speckle object beam has an amplitude $A_0 = |A_0| \exp[i(\psi_0 + \phi_0)]$, where the total phase is split into two parts. ϕ_0 is a slowly varying function of position across the object, and ψ_0 is a spatially rapidly varying function corresponding to the randomly added phase of each speckle upon ϕ_0. The phase is split into two parts so that the high-frequency speckles can be ensemble averaged to find the functional form of the speckle-correlation fringes. When the object and the reference beams are combined in the interferometer, the resulting slowly varying phase difference is defined as $\phi = \phi_0 - \phi_R$. These amplitudes and phases are functions of x and y, the position across the image of the speckle-producing object. When deformations are observed, the phase of the speckle field after perturbation of the object is changed by a $\Delta\phi(x, y)$, and the object-field complex amplitude becomes $A_0' = |A_0| \exp[i(\psi_0 + \phi_0 + \Delta\phi)]$.

For a single data frame, the intensity incident upon the detector in an ESPI system is given by the interference equation

$$I(x, y, t) = |A_0(x, y)|^2 + |A_R(x, y)|^2 + 2|A_0(x, y)||A_R(x, y)| \times \mathrm{Re}(\exp\{i[\psi_0(x, y) + \phi_0(x, y, t) - \phi_R(x, y, t)]\}). \tag{2}$$

This equation assumes that the amplitudes of the self-interference of the reference and the object beams are independent of time. The cross interference between the two beams depends on time through the optical phase difference, and the intensity recorded by the camera is an average over the integration time of the camera. For time-averaged vibrations, many periods of the object vibration are contained within the camera's integration time. Pulling out the time-dependent phase terms, the functional form of the resulting secondary fringes is denoted by the fringe function for the nth frame, M_n. With time-independent amplitudes, this is defined as

$$M_n(x, y) = \int \exp[i\phi_{Rn}(x, y, t) - i\phi_{0n}(x, y, t)]\mathrm{d}t. \tag{3}$$

This function contains what changes in time, whether for a sinusoidally vibrating object or a stepwise change between exposures in double-exposure measurements. After the speckle pattern has been recorded, dc filtered, rectified, and square law detected, the resulting monitor brightness for the nth speckle frame can be written as[7,9]

$$B_n(x, y) = a_n{}^2[|A_0(x, y)|^2 + |A_R(x, y)|^2 + 2\,\mathrm{Re}[A_R{}^*(x, y)A_0(x, y)M_n(x, y)] + N_n(x, y)]^2, \tag{4}$$

where a_n is a multiplicative coefficient, which will be set equal to 1 for this derivation. N_n is the electronic noise added to the speckle frame by the detection and processing electronics. After multiplying this expression out, an ensemble average of the brightness is performed to yield the expectation for the monitor brightness as a function of position x, y. The monitor brightness then becomes

$$\begin{aligned}\langle B(x, y)\rangle &= \langle I_R\rangle^2 + \langle I_0\rangle^2 + 4\langle \mathrm{Re}[(A_R{}^*A_0)^2]\rangle|M|^2 + \langle N^2(x, y)\rangle \\ &= \langle I_R\rangle^2 + \langle I_0\rangle^2 + 4\langle I_R I_0\rangle\langle\cos^2(\psi_0)\rangle|M|^2 + \langle N^2\rangle \\ &= \langle I_R\rangle^2 + \langle I_0\rangle^2 + 2\langle I_R\rangle\langle I_0\rangle|M|^2 + \sigma_e{}^2, \end{aligned} \tag{5}$$

where angle brackets denote ensemble averages. This expression assumes that (1) the electronic noise is a Gaussian distribution and statistically independent from the optical signal, (2) the reference and the object fields are independent of each other, and (3) the object-field amplitude obeys circular-Gaussian statistics in the complex plane, which leads to the statistical independence of the intensity and the phase in the object field.[13] Thus the signal-to-noise ratio is

$$\alpha_I = \frac{S}{N} = \frac{2|M(x, y)|^2\langle I_R\rangle\langle I_0\rangle}{\langle I_R\rangle^2 + \langle I_0\rangle^2 + \sigma_e{}^2}, \tag{6}$$

where $\sigma_e{}^2 = \langle N^2\rangle$.

The signal-to-noise ratio derived above is for the case of detecting a single speckle pattern. This process is applicable to the traditional method of observing time-averaged vibrations. By dc filtering, most of the self-interference terms can

be removed when the reference-to-object-beam intensity ratio is optimized.[9]

Another process used in ESPI is that of subtracting two speckle patterns to yield secondary fringes corresponding to the deformation of the object between the recording of the two speckle patterns. Furthermore, the subtraction of two speckle patterns removes self-interference terms and can be applied to the observation of time-averaged vibrations in order to enhance fringe contrast. The signal-to-noise ratio for subtraction can be determined by using the same assumptions as the single-frame case. When two speckle patterns are subtracted, the subtraction must take place before the squaring and averaging. This process yields a monitor brightness equal to

$$B(x,y) = \sum_{n=1}^{2} \{a_n[I_n(x,y) + N_n(x,y)]\}^2, \tag{7}$$

where I_n is given by the interference equation [Eq. (2)]. Expanding this for subtraction with $a_1 = 1$ and $a_2 = -1$ yields

$$\begin{aligned} B(x,y) = (&\{I_{R1}(x,y) + I_{01}(x,y) + 2\,\mathrm{Re}[A_{R1}{}^*(x,y) \\ &\times A_{01}(x,y)M_1(x,y)] + N_1(x,y)\} \\ &- \{I_{R2}(x,y) + I_{02}(x,y) \\ &+ 2\,\mathrm{Re}[A_{R2}{}^*(x,y)A_{02}(x,y)M_2(x,y)] \\ &+ N_2(x,y)\})^2. \end{aligned} \tag{8}$$

Since I_R and I_0 are time independent, we can also assume that they will not change between the two recorded speckle patterns. This can be done because the object motion between the two frames of data should be small compared with the wavelength. The I_R and I_0 terms will then cancel each other. The electronic noise terms vary from one frame to the next and therefore will not cancel each other. Hence Eq. (8) can be significantly reduced to give

$$\begin{aligned} B(x,y) = (&2\,\mathrm{Re}\{A_R{}^*(x,y)A_0(x,y)[M_1(x,y) - M_2(x,y)]\} \\ &+ [N_1 - N_2])^2. \end{aligned} \tag{9}$$

This expression is then expanded and ensemble averaged using the same statistical assumptions as the single-frame procedure to yield

$$\begin{aligned} \langle B(x,y)\rangle &= 4\langle \mathrm{Re}[(A_R{}^*A_0)^2]\rangle |M_1(x,y) - M_2(x,y)|^2 \\ &\quad + \langle (N_1 - N_2)^2\rangle \\ &= 4\langle I_R I_0\rangle \langle \cos^2(\psi_0)\rangle |M_1(x,y) - M_2(x,y)|^2 \\ &\quad + \langle N_1{}^2\rangle + \langle N_2{}^2\rangle \\ &= 2\langle I_R\rangle \langle I_0\rangle |M_1(x,y) - M_2(x,y)|^2 + 2\sigma_e{}^2, \end{aligned} \tag{10}$$

which will give a signal-to-noise ratio of

$$\alpha_{II} = \frac{|M_1 - M_2|^2 \langle I_R\rangle \langle I_0\rangle}{\sigma_e{}^2}. \tag{11}$$

There are many differences between this equation and Eq. (6). This equation has twice the noise as Eq. (6) for a single frame with the same amount of signal. The denominator for the two-frame situation depends only on the electronic noise, whereas the denominator in Eq. (6) includes the self-interference noise terms. Another difference is the maximum signal-to-noise ratio possible with the two techniques. To illustrate this, let the signal that will maximize α [in Eq. (6)] be $M(x,y) = 1$ to yield $|M(x,y)|^2 = 1$. Then, for the subtraction case, a maximum for α occurs when $M_1(x,y) = 1$ and $M_2(x,y) = -1$ yielding $|M_1(x,y) - M_2(x,y)|^2 = 4$. Thus, when the self-interference terms in the denominator of Eq. (6) are neglected, the maximum signal-to-noise ratio for the subtraction case will be twice that for the single frame. But, in practice, for the single-frame case, the self-interference terms will limit the performance of the system and thereby reduce the signal-to-noise ratio.

The expression of interest for the analysis of different time-averaged vibration-observation techniques is $|M_1 - M_2|^2$. This expression is proportional to the signal in Eq. (11) and will be referred to as the monitor, or secondary, fringe function. It will be normalized so that the signal covers the entire dynamic range of the monitor and evaluated for five different vibration techniques. This will require the noise to be scaled also by the same factor, so that the signal-to-noise ratio is unchanged.

Case I

This is the method traditionally used to observe vibrations with ESPI and directly corresponds to holographic-interferometry techniques for vibration analysis.[14] In this case, a single frame of the time-averaged speckle pattern is recorded, dc filtered, rectified, and then squared. Assuming a sinusoidally vibrating object, this object has a phase

$$\psi(x,y,t) = \exp\left\{i\left[\phi(x,y) - \frac{4\pi a_0}{\lambda}\cos(\omega t)\right]\right\},$$

where ϕ is the time-independent phase difference between the object and the reference beams, a_0 is the vibration amplitude, ω is the vibration frequency, and λ is the wavelength of the illumination. The fringe function M is then

$$\begin{aligned} M(x,y) &= \left(\frac{1}{T}\right)\exp[i\phi(x,y)] \int_0^T \exp\left[\frac{i4\pi a_0}{\lambda}\cos(\omega t)\right] dt \\ &= \exp(i\phi) J_0\left(\frac{4\pi a_0}{\lambda}\right), \end{aligned} \tag{12}$$

where J_0 is a zero-order Bessel function. The monitor fringe function is then the square of a zero-order Bessel function,

$$2|M(x,y)|^2 = J_0{}^2\left(\frac{4\pi a_0}{\lambda}\right). \tag{13}$$

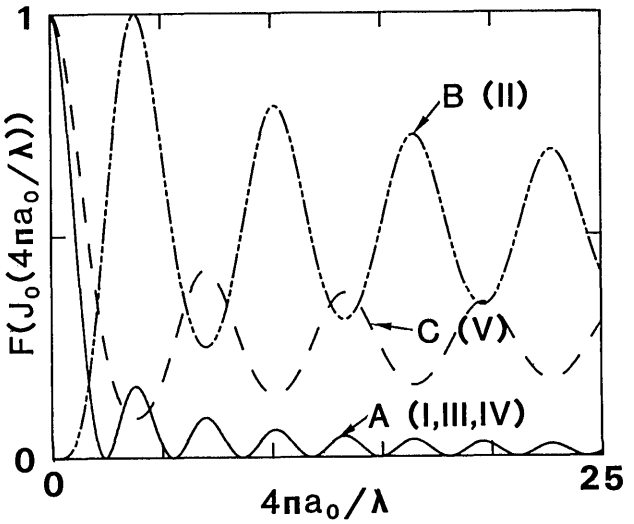

Fig. 1. Plots of functions of Bessel functions. A, $J_0{}^2(4\pi a_0/\lambda)$ for Cases I, III, and IV. B, $[1/1.968][1 - J_0(4\pi a_0/\lambda)]^2$ for Case II. C, $[1/4][1 + J_0(4\pi a_0/\lambda)]^2$ for Case V.

The factor of 2 on the left-hand side of this equation comes from the numerator of Eq. (6). This factor is needed to compare the fringe contrast of this method with the rest of the methods presented. The fringe maxima and minima are calculated using the signal (numerator) and noise (denominator) expressions shown in Eqs. (6) and (11). It is assumed that the average intensity of each beam is unity and that the self-interference terms are not present. This function is plotted as curve A in Fig. 1.

Case II

In this case, a reference frame recorded with the object at rest is continually subtracted from the time-averaged data. Like Case I, this technique has a counterpart in holography known as real-time holographic interferometry.[15] It has been used for speckle-interferometry measurements by Nakedate *et al.*[16] However, their analysis failed to account for the existence of additive electronic noise. The reference frame has a fringe function $M_1 = \exp(i\phi)$, and the data frame has the fringe function $M_2 = \exp[i(\phi + \Delta\phi)]J_0(4\pi a_0/\lambda)$, where $\Delta\phi$ is a possible phase change between the reference and the data frames that may be caused by slow object drift. When combined and normalized, the secondary fringes become

$$|M_1 - M_2|^2 = \frac{1}{1.968}\left[1 - 2J_0\left(\frac{4\pi a_0}{\lambda}\right)[\cos(\Delta\phi)] + J_0^2\left(\frac{4\pi a_0}{\lambda}\right)\right]. \tag{14}$$

Note that the quantity in brackets is a function of a Bessel function, has a minimum value of 0, and damps off to a value of 1. Equation (14) has been normalized so that the signal will fall between 0 and 1 over the full dynamic range of the monitor, with $\langle I_R\rangle\langle I_0\rangle = 1$. Thus vibration nodes will appear to be dark, and subsequent fringe orders will have a minimum greater than 0 and modulate about a value of 1. The cosine factor will cause an additional set of fringes owing to decorrelation effects, which will appear on top of the vibration fringes if the object slowly drifts or distorts. Because both exposures contain the cross interference between the object and the reference beams, the cross-interference terms both add and subtract from each other when the time-averaged frames are subtracted. As long as the object is stable, $\Delta\phi$ can be considered to be very small, so that

$$|M_1 - M_2|^2 = \frac{1}{1.968}\left[1 - J_0\left(\frac{4\pi a_0}{\lambda}\right)\right]^2. \tag{15}$$

Since the object may not be stable always, this is not the best way to observe vibrations in time. This function is plotted as curve B in Fig. 1. The electronic noise in this case is twice as much as that in Case I because two data frames are involved instead of one; however, it is scaled by the same value as the fringe function. This leaves the noise at a value slightly higher than the single-frame case.

Case III

This is the new method that is presented in this paper. A reference frame is recorded while the object is at rest, with a reference mirror vibrated at a large amplitude—or an amplitude corresponding to a zero of the J_0^2 function—to eliminate the cross-interference term and leave only self-interference noise terms. This reference frame is then repeatedly subtracted from the time-averaged data frames taken with the object vibrating and the reference mirror still. The reference frame could be created by adding exposures of each beam individually; however, this does not work so well because the object beam is very weak in comparison with the reference beam and will not cover the dynamic range of the camera. The amplitude of vibration for the reference mirror is chosen such that $M_1 = 0$. With $M_2 = \exp(i\phi)J_0(4\pi a_0/\lambda)$, the monitor fringe function is

$$|M_1 - M_2|^2 = J_0^2\left(\frac{4\pi a_0}{\lambda}\right). \tag{16}$$

Since the secondary fringe falls between 0 and 1, Eq. (16) need not be scaled. Thus this is the same function as that for Case I; however, the electronic noise will be four times that of Case I because two data frames are involved. With this technique there will be no residual self-interference terms left to reduce the visibility of the fringes. There will be self-interference residuals in Case I, unless a specially designed double-slit aperture is used that reduces the cross-interference bandwidth and the amount of light available.[17] Thus this method is much better than that of Case I, even though there is four times the amount of noise after normalization. This function is plotted as curve A in Fig. 1.

Case IV

At this point, we would like to find the fringe functions for other possible vibration techniques. The first method involves creating a reference frame with the vibrating object in motion. This time-averaged frame is then repeatedly subtracted from other time-averaged speckle patterns of the object, which have the phase of one beam shifted by π with respect to the other. For the first frame $M_1 = \exp(i\phi)J_0(4\pi a_0/\lambda)$, and for the second frame $M_2 = \exp[i(\phi + \Delta\phi + \pi)]J_0(4\pi a_0/\lambda)$. Then, including a normalization factor,

$$|M_1 - M_2|^2 = \left(\frac{4}{4}\right)J_0^2\left(\frac{4\pi a_0}{\lambda}\right)\cos^2\left(\frac{\Delta\phi}{2}\right) = J_0^2\left(\frac{4\pi a_0}{\lambda}\right)\cos^2\left(\frac{\Delta\phi}{2}\right), \tag{17}$$

where $\Delta\phi$ is a phase difference between the two frames. $\Delta\phi$ is a function of x and y and may be slowly varying in time. The cross-interference terms should again cancel each other, but, if there is any object motion between the two exposures, a second set of fringes will appear on top of the vibration fringes because of object movement. The cross-interference terms can then add to each other to account for the factor of 4 in the numerator of Eq. (17). The 4 in the denominator is a normalization factor. As long as the object is stable, $\Delta\phi$ should be very small. But if the object drifts in time and shows some instability, this method will not work well. After scaling, the electronic noise will be one half that for the single frame. For a stable object, this case will have a normalized monitor fringe function equivalent to that in Cases I and III.

Case V

This is the last variation to be covered in this paper. By recording a reference frame with the object at rest and then shifting the phase of one beam by π before recording the time-averaged data frame, the node of the vibration pattern will be bright. This technique is similar to that of Nakedate *et al.*[16] (Case II), except that the π phase shift enables the

fringe pattern to have bright nodal regions instead of dark ones. The reference-frame fringe function is $M_1 = \exp(i\phi)$, and the data-frame fringe function equals $M_2 = \exp[i(\phi + \Delta\phi + \pi)]J_0(4\pi a_0/\lambda)$. When combined and normalized, the fringe function seen on the monitor becomes

$$|M_1 - M_2|^2 = \frac{1}{4}\left[1 + 2J_0\left(\frac{4\pi a_0}{\lambda}\right)\cos(\Delta\phi) + J_0^2\left(\frac{4\pi a_0}{\lambda}\right)\right]. \quad (18)$$

This outcome is also dependent on object stability. An extra set of fringes that are due to decorrelation will affect the viewed vibration fringes if the object drifts at all. The secondary-fringe function denoted by the quantity in the brackets has a maximum value of 4 at the zero-order mode and will damp down to a value of 1 as in Case II. For a stable object, Eq. (18) may be rewritten as

$$|M_1 - M_2|^2 = \frac{1}{4}\left[1 + J_0\left(\frac{4\pi a_0}{\lambda}\right)\right]^2. \quad (19)$$

The electronic noise in this case will again be one half that for the single frame after normalization. This function is plotted as curve C in Fig. 1.

3. CALCULATION OF CONTRAST

Comparison of the normalized secondary fringe functions for Cases I through V is best done by looking at fringe contrast. The contrast defined by Eq. (1) in terms of the maximum and the minimum values of intensity can be used to calculate the contrast without an explicit formula. The local contrast is defined to be the contrast as calculated from Eq. (1) using an adjacent maximum and minimum of the fringe function. A computer program was written to evaluate and plot the contrast of the monitor fringe functions. This calculation accounts for electronic noise by setting the minimum equal to the noise if the signal plus noise was less than the noise. The maximum values are equal to the local maximum signal plus the noise. These calculations neglect the presence of self-interference terms as well as decorrelation of the cross-interference term between frames. The self-interference terms reduce the contrast of Case I when they are larger in magnitude than the electronic noise. The decorrelation among data frames causes extraneous fringes that are due to object drift, which severely reduces vibration fringe visibility.

The electronic noise in each of the five cases will be normalized by the same factors that scaled the secondary-fringe functions. The signal and the noise measured by the camera are processed together before displaying. When displayed, the processed data are scaled to fit within the dynamic range of the monitor by adjusting the monitor gain or by scaling the data in a computer. For a given electronic-noise value σ_e^2, the noise used in the contrast calculations N will have the following values:

Cases I, IV, V	$N = \sigma_e^2/2$,
Case II	$N = \sigma_e^2/1.968$,
Case III	$N = 2\sigma_e^2$.

These values assume that the average beam intensities are unity and that the self-interference terms are zero. Again, this noise is normalized such that the signal covers the monitor's dynamic range. Therefore it will affect the signal-to-noise ratio viewed on the monitor as well as the fringe contrast.

Plots of the monitor fringe contrast with no electronic noise for Cases I through V are shown in Fig. 2. The contrast for Cases I, III, and IV is equal to 1 if no noise is present because the function minima are zero. Cases II and V have decreasing contrast with vibration amplitude because the minima are nonzero. These last two cases have similar values for contrast.

Real-world systems inherently have electronic noise. Typically, the self-interference terms in an ESPI system can be reduced sufficiently so that 50 orders of the zero-order Bessel function may be observed. This would correspond to a noise value of $\sigma_e^2 = 0.004$ out of a maximum of 1.0. Figure 3 shows fringe contrast plots with this amount of noise. The highest contrast is the single time-averaged frame, but this assumes that any self-interference noise present is within σ_e^2. Case III shows a significantly larger contrast throughout the entire vibration amplitude range than do Cases II and V. This

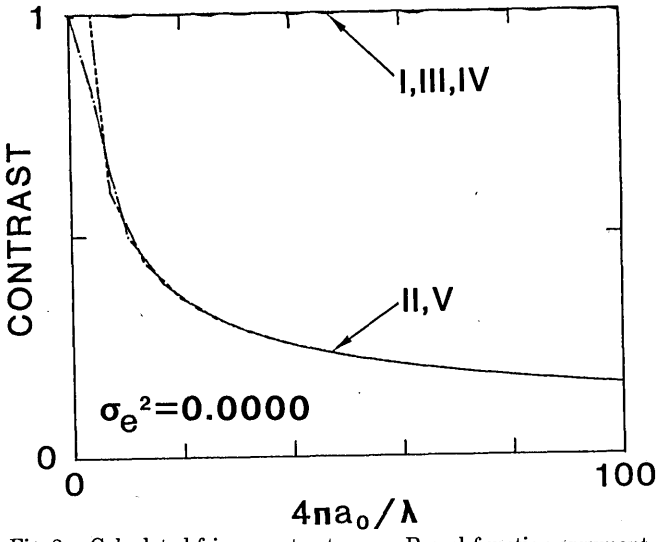

Fig. 2. Calculated fringe contrast versus Bessel-function argument ($4\pi a_0/\lambda$) with no electronic noise ($\sigma_e^2 = 0.000$) for the five vibration-observation techniques discussed.

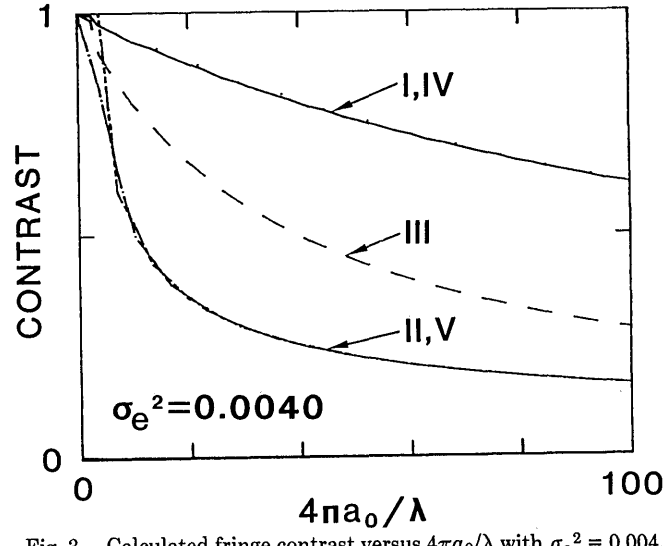

Fig. 3. Calculated fringe contrast versus $4\pi a_0/\lambda$ with $\sigma_e^2 = 0.004$. This amount of noise enables 50 J_0^2 fringes to be viewed.

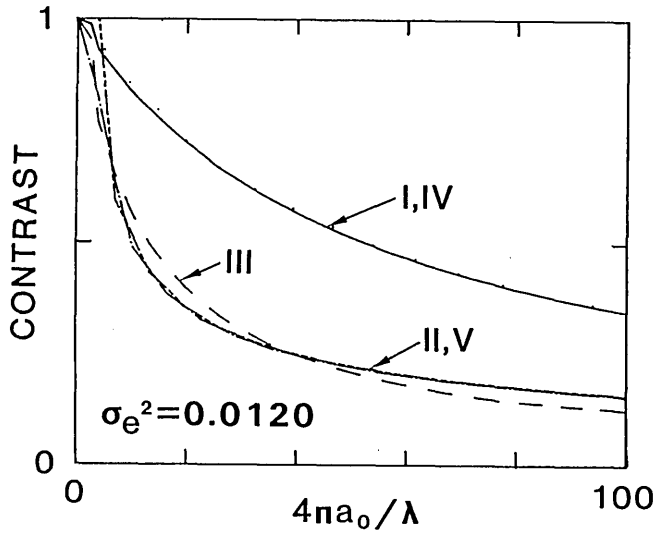

Fig. 4. Calculated fringe contrast versus $4\pi a_0/\lambda$ with $\sigma_e^2 = 0.012$.

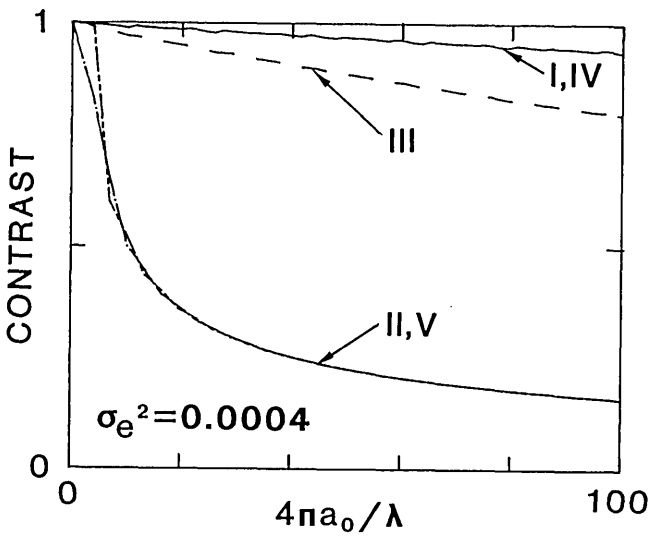

Fig. 5. Calculated fringe contrast versus $4\pi a_0/\lambda$ with $\sigma_e^2 = 0.0004$. This is the amount of noise present in the DSPI system described in this paper.

assumes that there is no object drift between frames to produce decorrelation fringes that would reduce monitor fringe contrast.

For Case III to have contrast comparable with that of Cases II and V, the electronic noise would have a value of about 0.012 (Fig. 4). This would correspond to being able to observe about 16 fringes in the optimized single-frame time-averaged case. For Cases I and IV to have contrast comparable with that of Cases II and V, the electronic noise would have to be as large as 0.05.

The noise was measured in our DSPI system by finding the rms of the difference between two subtracted frames. This procedure will functionally yield $\sqrt{2}\sigma_e$. The measured value of σ_e^2 is 0.0004, which corresponds to viewing 500 fringes of the J_0^2 function. This is 1 order of magnitude better than most TV-camera systems. Contrast plots for this value of electronic noise are shown in Fig. 5. The curves for Cases III and IV are quite good. Cases II and V have much lower contrasts. In all these plots, Cases II and IV have approximately the same values independent of the noise values.

In comparing the contrast results for the five cases, practical problems tend to reduce these optimistic predictions. For Case I, the biggest limitation is optimization of the self-interference terms. Ideally, the electronic noise should limit performance, but, in practice, the self-interference noise does. Cases II, IV, and V will not yield the calculated results if the object is at all unstable over the time period between exposing the reference and the data frames. As the object drifts in time, the cross-interference term in the data frame will depart from the one recorded in the reference frame. This phenomenon will result in the appearance of a second set of fringes that is due to decorrelation modulating the vibration fringes. These decorrelation fringes will also have higher contrast than the vibration fringes, so that it will be difficult to determine the location of the vibration fringes. Case III will not be influenced by object drift, since there is no cross-interference term contained in the reference frame. Having a reference frame containing noise terms relaxes the need to optimize the values of the self-interference terms as in Case I. Thus the reference-to-object-beam ratio is less critical.[1] The self-interference terms will cancel in Case III, but the electronic noise will not cancel. Examples of experimental results using the methods of Case I and Case III are given in Section 4.

4. EXPERIMENTAL RESULTS

The DSPI utilized for these experiments includes a Reticon 100 × 100 diode-array camera interfaced to an HP-9836C desktop computer. The light source is a 10-mW He–Ne laser. A schematic of the system is shown in Fig. 6. The reference beam is a spherical wave produced by a single-mode optical fiber mounted at the center of the aperture stop. The object beam is collimated and illuminates a diffuse object. The object is then imaged onto the detector array by means of a lens through the limiting aperture where the fiber is mounted. This limiting aperture determines the speckle size at the detector array. For this type of interferometer, the speckles must be resolved. Thus, for a 60-μm detector element spac-

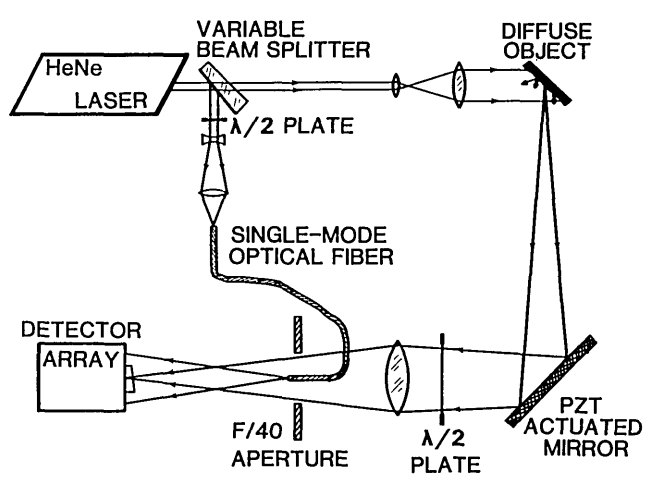

Fig. 6. Schematic of a DSPI. The reference beam consists of a single-mode optical fiber placed in the center of the aperture that produces a specular spherical wave. The object beam is collimated and illuminates a diffuse object that is then imaged onto a detector array. The object is excited by an attached PZT. The PZT-actuated mirror is used to create a reference frame in Case III.

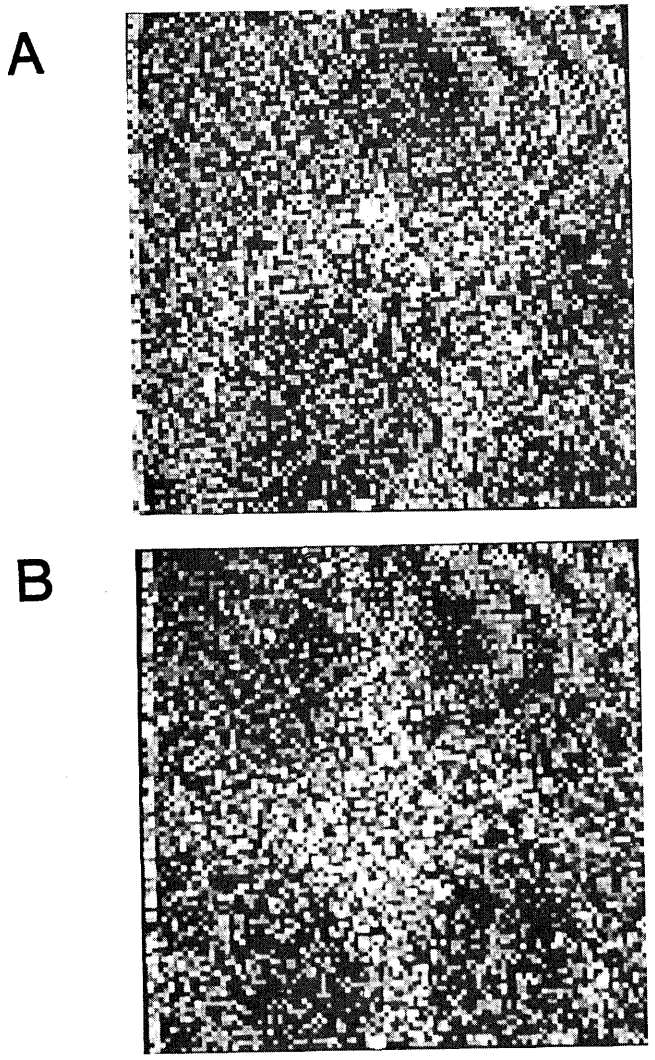

Fig. 7. Vibration fringes observed using a single frame of data that has been high-pass filtered and squared before displaying. The object is a steel plate clamped on one side with a PZT exciting the other end. A, 7300-Hz resonance; B, 8560 Hz.

ing, the beam must be about $F/39$. The object used in this experiment is a thin rectangular steel plate coated with silver paint. This steel plate is bound on one end to a post and excited at the other end by a piezoelectric transducer (PZT). It is not truly a Lambertian surface but is nearly specular to conserve light. The diode array passes data into an electronic interface that digitizes to 8 bits. The integration time of the array may vary from 5 to 20 msec. For this experiment, the integration time was set at 5 msec, which is considerably shorter than the 33- to 40-msec standard TV rates.

The single-mode fiber produces a clean spherical wave front and does not block much of the object beam. Random fiber motion because of air currents changes the phase slightly at the image plane but does not disturb fringe visibility when the system is on an isolated bench; however, when averaging many sets of data, the system must be enclosed.

The most important consideration in aligning the system is the need to have equal path lengths for the object and the reference beams so that the cross-interference term between the two beams is present. Another consideration is to make sure that both beams have the same polarization orientation at the detector surface if the fiber output is polarization dependent. This can be ensured by placing $\lambda/2$ plates in the object beam and before the fiber coupler.

The reference-to-object-beam ratio should be optimized to maximize the cross interference between the two beams. This is done by observing each beam after it has been high-pass filtered and squared. This processing yields the residual self-interference noise in each beam. The self-interference noise terms in both beams should be about equal to maximize cross interference. The sum of the two self-interference patterns will be the darkest part of the single-vibration fringe patterns, and the cross interference between the two beams will be the brightest areas.

Figure 7 shows the results of filtering[1] and squaring a time-averaged vibration frame inside the computer (Case I). These photographs show two resonant modes of the steel plate. The bright areas are the nodes, and the dark parts of the fringes are noisy. This is due to self-interference noise.

In contrast, Fig. 8 shows the results of using a reference frame that contains only the unwanted self-interference noise without the cross interference (Case III) with the same object

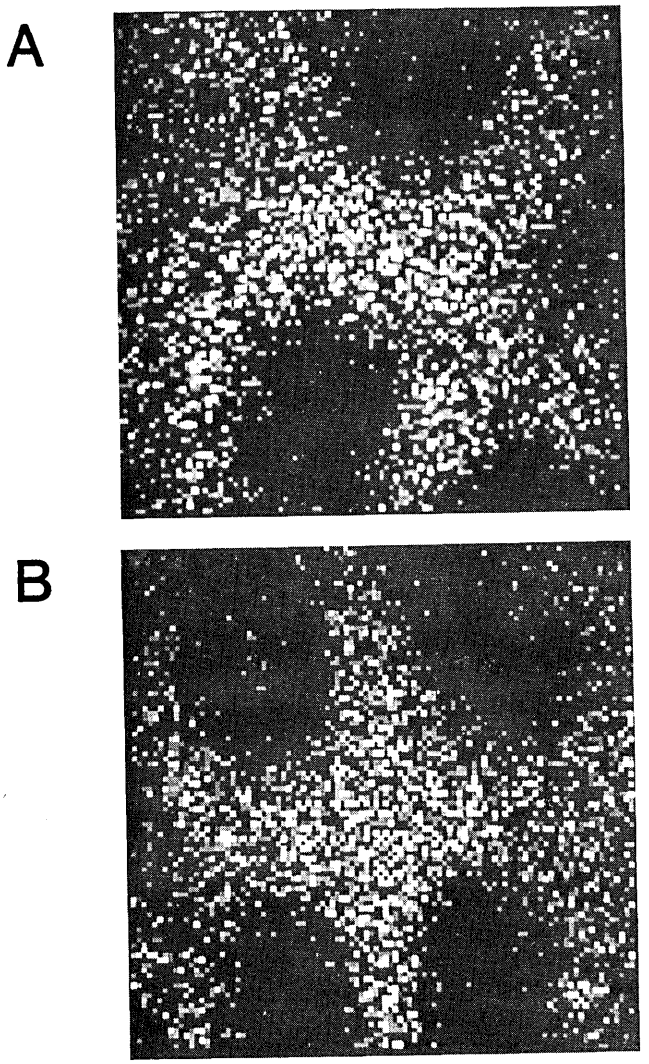

Fig. 8. Vibration fringes observed by the method outlined in Case III. Same object and resonances as Fig. 7. Noise terms have been subtracted out using a reference frame created by vibrating a PZT-driven mirror at 800 Hz with object at rest (see Fig. 6).

resonances. The reference frame is created by sinusoidally vibrating a mirror excited by a PZT with a large amplitude while the object is at rest (see Fig. 6). It is assumed that the mirror does not tilt as it is translated. Since the reference mirror is located in the object beam, any tilt in the movement of the reference mirror could distort the recorded self-interference of the object beam. If the mirror tilts, the self-interference may not completely subtract out as wanted. This reference frame is continually subtracted from time-averaged vibration data frames. The difference is then squared and displayed. Using this method of processing significantly enhances the fringe contrast (Fig. 8). The nodal areas are just as bright, but the dark areas are dark and limited only by electronic noise. The self-interference terms have been subtracted out. The object used to obtain the fringes in Figs. 7 and 8 was too unstable for recognizable fringes to be viewed using the methods of Cases II, IV, and V.

5. CONCLUSIONS

DSPI and ESPI are convenient ways to observe vibration fringes. Many different techniques of processing these fringes can be used. All these techniques have a processed monitor fringe function that is a second-order function of a zero-order Bessel function. The easiest fringes to interpret are those that have the J_0^2 dependence (Cases I, III, and IV). This function has bright areas where the object is stationary, dark areas that go to zero, and secondary fringes that damp in amplitude. The other functional forms (Cases II and V) have fringes that oscillate about a fixed intensity level and never damp to zero and possibly dark areas corresponding to vibration nodes (Case II). These other functional forms also have lower contrasts than the J_0^2 form for reasonable amounts of electronic noise.

The best technique to use depends on the processing speed, the amount of electronic and self-interference noise, and the stability of the object under test. With the DSPI system, high-pass filtering is not fast. However, subtraction can be done much faster. The system described here will process up to two frames per second. ESPI systems using analog processing can use TV rates. However, a DSPI system can have hard-wired processing to increase the speed. With self-interference noise smaller in magnitude than electronic noise, the filtering of a single frame of data will permit 50 fringes to be viewed. This is more than enough for most applications. If the self-interference noise is larger than the electronic noise, subtraction techniques can enhance the fringe contrast by eliminating the self-interference terms. For highly stable objects, all the subtraction techniques will take care of the self-interference noise. If subtraction techniques are used for highly unstable objects, decorrelation of the self-interference terms between the reference and the data frames is bound to occur, and the self-interference terms will not cancel in the subtraction process. With highly unstable objects, single time-averaged data frames are better because they are updated faster, and no reference frame is used. If the object is moderately unstable, subtraction using a reference frame containing only self-interference noise terms will significantly enhance fringe contrast. This type of reference frame ensures that decorrelation fringes will not appear because of object drift. Use of this method provides a technique for observing high-contrast fringes of vibrating objects that may drift or distort slowly in time.

ACKNOWLEDGMENT

One of the authors acknowledges support from Hughes Aircraft Company for part of this research, and we thank Jim Wyant for his helpful discussions and encouragement.

REFERENCES

1. K. Creath, "Digital speckle pattern interferometry (DSPI) using a 100 100 imaging array," Proc. Soc. Photo-Opt. Instrum. Eng. **501**, 292 (1984).
2. J. N. Butters and J. A. Leendertz, "Speckle pattern and holographic techniques in engineering metrology," Opt. Laser Technol. **3**, 26 (1971).
3. A. Macovski, S. D. Ramsey, and L. F. Schaefer, "Time-lapse interferometry and contouring using television systems," Appl. Opt. **10**, 2722 (1971).
4. R. Jones and C. Wykes, "General parameters for the design and optimization of electronic speckle pattern interferometers," Opt. Acta **28**, 949 (1981).
5. C. Wykes, "Use of electronic speckle pattern interferometry (ESPI) in the measurement of static and dynamic surface displacements," Opt. Eng. **21**, 400 (1982).
6. R. Jones and C. Wykes, *Holographic and Speckle Interferometry* (Cambridge U. Press, Cambridge, 1983).
7. G. Å. Slettemoen, "General analysis of fringe contrast in electronic speckle pattern interferometry," Opt. Acta **26**, 313 (1979).
8. O. J. Løkberg, "Advances and applications of electronic speckle pattern interferometry (ESPI)," Proc. Soc. Photo-Opt. Instrum Eng. **215**, 92 (1980).
9. O. J. Løkberg and G. Å. Slettemoen, "Electronic speckle pattern interferometry," in *Applied Optics and Optical Engineering*, R. R. Shannon and J. C. Wyant, eds. (Academic, New York, to be published).
10. A. E. Ennos, "Speckle interferometry," in *Laser Speckle and Related Phenomena*, J. C. Dainty, ed. (Springer-Verlag, Berlin, 1975).
11. G. Å. Slettemoen, "Optimal signal processing in electronic speckle pattern interferometry," Opt. Commun. **23**, 213 (1977).
12. R. Jones and C. Wykes, "De-correlation effects in speckle-pattern interferometry. 2. Displacement dependent de-correlation and applications to the observation of machine-induced strain," Opt. Acta **24**, 533 (1977).
13. J. W. Goodman, "Statistical properties of laser speckle patterns," in *Laser Speckle and Related Phenomena*, J. C. Dainty, ed. (Springer-Verlag, Berlin, 1975).
14. R. L. Powell and K. A. Stetson, "Interferometric vibration analysis by wavefront reconstruction," J. Opt. Soc. Am. **55**, 1593 (1965).
15. K. A. Stetson and R. L. Powell, "Interferometric hologram evaluation and real-time vibration analysis of diffuse objects," J. Opt. Soc. Am. **55**, 1694 (1965).
16. S. Nakedate, T. Yatagai, and H. Saito, "Digital speckle-pattern shearing interferometry," Appl. Opt. **24**, 4241 (1980).
17. K. Biedermann and L. Ek, "A recording and display system for hologram interferometry with low resolution imaging devices," J. Phys. E **8**, 571 (1975).